Inter-element phase self-calibration for GIMS (geostationary interferometric microwave sounder) postprint

Authors: Han, Donghao, Liu, Hao, Wu, Ji, Zhang, Cheng

Date: 2017-03-10T00:00:00+00:00

Abstract

The inter-element phase calibration plays an important role in the overall calibration scheme for synthetic aperture radiometer. The traditional relative phase calibration approach is to use correlated noise injection network, which will be difficult to be implemented in millimeter wave band due to the complexity of the waveguide divider network. A novel self-calibration method for interferometric radiometers with rotating thinned array, especially for the geostationary interferometric microwave sounder(GIMS), has been proposed in this paper. By using this approach, neither dedicated hardware nor dedicated calibration working model is needed to achieved the relative phase calibration. The self-calibration approach is inherently merged with the nominal observation working model of GIMS, thanks to the continuous array rotating of GIMS instrument. A running average scheme has been introduced into the self-calibration approach to enhance the SNR of the calibration data, which is normally very low with the natural earth scene. The method is demonstrated by both simulation and field imaging experiment. 2016 IEEE.

Full Text

Preamble

Inter-Element Phase Calibration for Geostationary Interferometric Microwave Sounder (GIMS)

Donghao Han, Hao Liu, Member, IEEE, Ji Wu, Fellow, IEEE, Zhang Cheng, Member, IEEE, Lijie Niu, Ying Zhang

Abstract—The Geostationary Interferometric Microwave Sounder (GIMS) is a new concept of atmospheric microwave sounder for China' s future geostationary *orbit meteorological satellite (FY-4). A novel self-calibration method for interferometric radiometers with rotating thinned array, especially for GIMS, has been proposed in this paper. Compared with traditional relative phase calibration approaches, neither dedicated hardware nor dedicated calibration working model is needed to achieve the relative phase calibration in this novel inter-element phase calibration. The self-calibration approach is inherently merged with the nominal observation working model of GIMS, thanks to the continuous array rotating of the GIMS instrument. A running average scheme has been introduced into the self-calibration approach to enhance the signal-to-noise ratio (SNR) of the calibration data, which is normally very low with natural Earth scene. The method is demonstrated by both simulation and field imaging experiment.*

Index Terms—inter-element phase calibration, Geostationary Interferometric Microwave Sounder (GIMS), phase error, synthetic aperture radiometer

I. INTRODUCTION

Realizing microwave sounding from geostationary Earth orbit (GEO) is an emerging research field since the 1990s [**?**][**?**]. GEO can guarantee fixed continuous observation of a particular region, while the relatively low frequency band (compared with infrared waves) can guarantee all-weather observation with 3D imaging capability for atmospheric temperature and moisture. These features make GEO microwave sounding very appealing for short-term meteorological forecasting.

The largest obstacle for GEO microwave observation is the restriction of spatial resolution. Interferometric aperture synthesis is an effective solution to this problem, using a thinned antenna array to replace a single large aperture antenna. Since the 2000s, several interferometry-based instrument concepts have been proposed, including the GeoSTAR concept by NASA/JPL [**?**], the GAS concept by ESA [**?**], and the GIMS concept by NSSC [**?**].

GIMS is a millimeter-wave imaging sounder concept proposed for China' s next-generation geostationary meteorological satellite (FY-4M). GIMS utilizes a rotating circular thinned array, instead of a stationary Y-shape array, to reduce the required number of antenna elements. A proof-of-concept 53 GHz ground-based GIMS demonstrator with 28 elements has been successfully developed and tested during 2009-2012 [**?**]. A new GIMS demonstrator development plan has been approved for further risk mitigation, with a 70-element demonstrator foreseen to be completed before the end of 2016. Fig. 1

illustrates the artistic view of the GIMS instrument in orbit.

Calibration of GIMS is a key process to ensure quantitative conversion of raw measurement data into scientific data with physical meaning. For GIMS, periodic single-element total power calibration can be easily achieved by a cold sky mirror and a blackbody installed on the fixed part of the platform with a deployable mechanism that can periodically switch to block the FOV of each

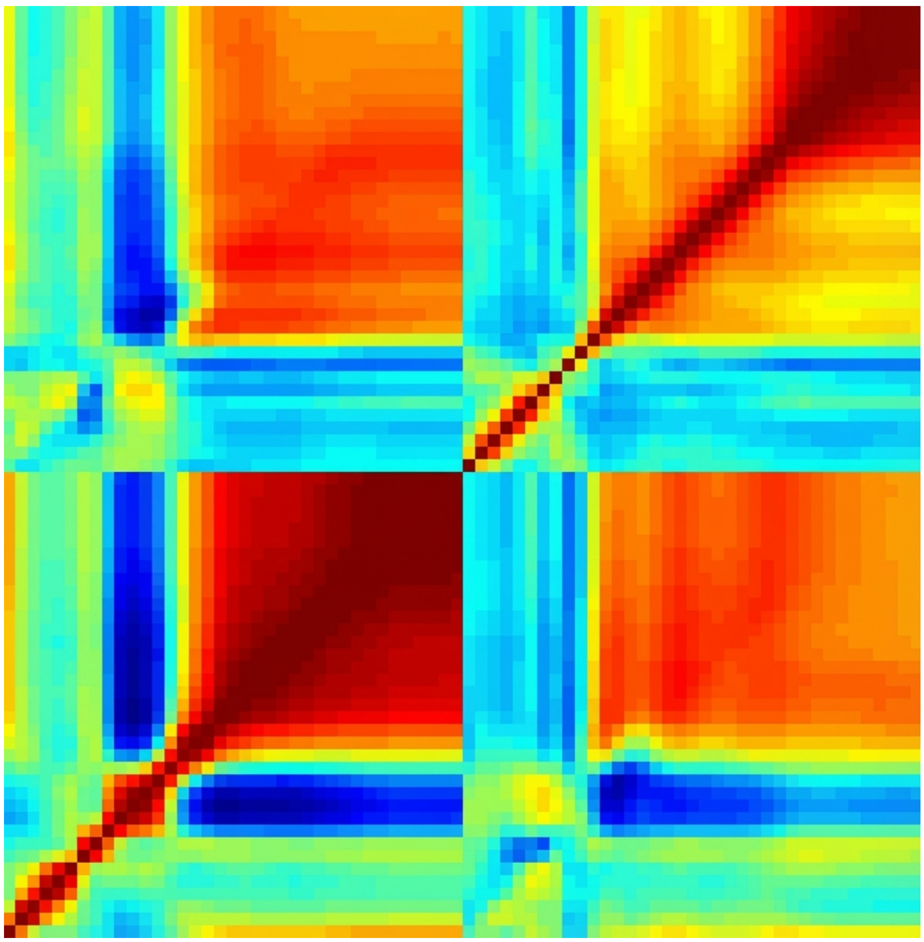

Figure 1: Figure 1

element antenna [?]. Besides single-element total power calibration, periodic inter-element phase calibration is also needed for an interferometric radiometer like GIMS. The traditional method uses correlated noise injection [?], which seriously increases hardware requirements and system complexity [?]. Different from this, some phase self-calibration methods have been proposed for GeoSTAR [?][?], in which specific extra external sources are necessary to improve measurement signal-to-noise ratio (SNR) during calibration [?].

In this paper, two new schemes have been introduced in the GIMS inter-element phase calibration method. First, thanks to array rotation, each baseline can obtain a conjugated measurement after half array revolution. Taking advantage of this feature, a running average scheme is proposed to reduce the effect of noise in phase calibration for GIMS, so extra point sources are no longer needed. Second, taking advantage of prior information of the brightness temperature distribution as viewed from geostationary orbit, the prior knowledge of the very short baseline phases is used to eliminate phase ambiguity. The practical inter-element phase calibration method has been set up for GIMS and demonstrated by both simulation and field imaging experiment.

II. GIMS INTER-ELEMENT PHASE MODEL

As a microwave interferometric radiometer (MIR), the thinned antenna array of GIMS with 70 elements is shown in Fig. 2

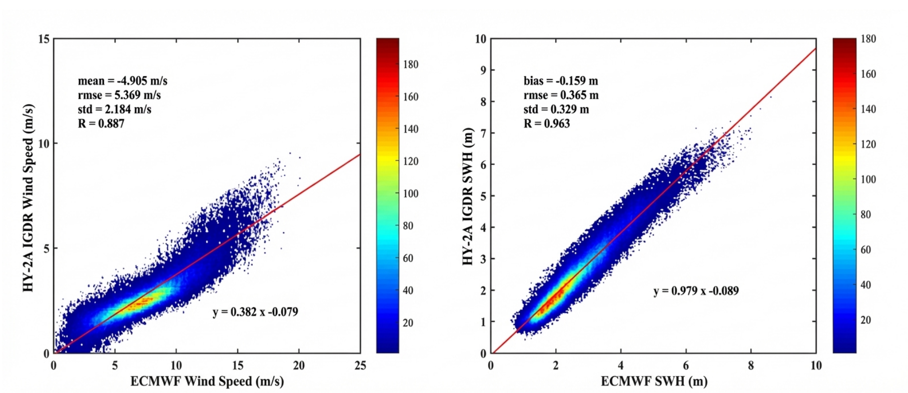

Figure 2: Figure 2

(a). Although the snapshot samples are very sparse and irregular, as shown in Fig. 2(b), full sampling coverage of the spatial frequency domain will be achieved after half revolution, which is also necessary for inter-element phase calibration.

The longest baseline of the array in Fig. 2 is about 617 , while the maximum spacing between two adjacent antennas is controlled under 130 , which is an important coefficient for inter-element phase calibration. Similar to the 28-element array of the proof-of-concept GIMS demonstrator [?], there are two kinds of antennas in the 70-element GIMS array: three small aperture antennas to form the shortest baselines, and 67 large aperture antennas to form other baselines. It should be pointed out that the second shortest antenna spacing is 6.3 , which is short enough to be preset with a confidence interval in the following sections.

The output of receivers is given by [?]:

$$V_{ij} = \psi_{ij} + \alpha_i - \alpha_j + \alpha_{ij}^n$$

where ψ_{ij} is the ideal phase of the visibility, α_i and α_j are the receiver phases, and α_{ij}^n is a random phase term introduced by thermal noise. α_{ij}^f is the inseparable phase error introduced by fringe washing, which can be considered negligible for the short and medium length baselines of GIMS. By running average scheme, which will be described in the following sections, α_{ij}^n can also be reduced to negligible. Then Eq. (2) can be further simplified as:

$$\phi_{ij} = \psi_{ij} + \alpha_i - \alpha_j$$

III. INTER-ELEMENT PHASE CALIBRATION

Lots of redundant information can be achieved during observation for GIMS, and element phase information will be implied in them. Inter-element phase calibration can extract this information through redundant observation in a reliable way.

A. Optimized Redundancy Equations

Image of the physical world has the property of real value when looking from space. Therefore, its ideal Fourier transformation is a Hermitian type function that has the property:

$$V(u, v) = V^*(-u, -v)$$

In which, asterisk means Hermitian operator. Image will be assumed changeless during one period of array rotation, then V_{ij}^{θ} and $V_{ij}^{\theta+\pi}$ are both measured by the same baseline with 180° baseline rotation. Submitting the phase information of (4) into (3), we can get [?]:

$$\begin{cases} \phi_{ij}^{\theta} = \psi_{ij}^{\theta} + \alpha_i - \alpha_j \\ \phi_{ij}^{\theta+\pi} = -\psi_{ij}^{\theta} + \alpha_i - \alpha_j \end{cases}$$

The superscript θ means baseline rotation angle. In which, u_{ij} and v_{ij} are the projections over the X-Y axes of the vector defined between the two phase centers of the antennas normalized to the wavelength. Subscript ij means channel number. (ξ, η) are the director cosines [?], (X, Y) equal axes, T_r is the receiver' s physical temperature [?][?], assumed equal in all elements. The phase of V_{ij}^{θ} and $V_{ij}^{\theta+\pi}$ are ϕ_{ij}^{θ} and $\phi_{ij}^{\theta+\pi}$ respectively. With a simple algebraic transformation:

$$\gamma_{ij}^{\theta} = \phi_{ij}^{\theta+\pi} - \phi_{ij}^{\theta} = -2\psi_{ij}^{\theta}$$

However, this procedure would yield large errors in the estimation of phases because the phase ψ_{ij}^{θ} presents a large error in most visibility samples due to very poor measurement SNR.

Running average scheme is proposed to optimize Eq. (6). Selecting an arbitrary time slice during the array rotation, we can get many pairs of γ_{ij}^{θ}. By averaging them:

$$\hat{\gamma}_{ij} = \frac{1}{N} \sum_{k=1}^{N} \gamma_{ij}^{\theta_k}$$

Eq. (12) is welcome to be added to Eq. (10), so the final redundancy equation is achieved:

$$\hat{\gamma}_{ij} = -2\psi_{ij}$$

where the superscript bracket means the optimization of ψ_{ij}. In which, θ_k is the rotation angle corresponding to the selected time slice. Eq. (7) implies that $\gamma_{ij}^{\theta_k}$ can be regarded as a measurement of ψ_{ij}, and $w_{ij}^{\theta_k}$ is the weight of this measure. Multiple measurements will be weighted averaged to improve measurement SNR, which can be defined as the ratio of visibility amplitude to the standard variation of noise.

From another point of view, running average scheme is equivalent to extending integration time, and the standard variation of noise is inversely proportional to the square of the integration time. So $\hat{\gamma}_{ij}$ can be optimized under the SNR optimization principle as:

$$\hat{\gamma}_{ij} = \frac{\sum_{k=1}^{N} w_{ij}^{\theta_k} \gamma_{ij}^{\theta_k}}{\sum_{k=1}^{N} w_{ij}^{\theta_k}}$$

With running average scheme, the measurement SNR will not be restricted by measurement amplitude, but the extent of selected time slice, which is limited by the instrument stability.

Taking all of the baselines into account for an array with N channels similarly as Eq. (7), the following set of equations can be established:

$$= \mathbf{P}$$

Phase ambiguity is produced by the division operation in Eq. (7), so the solution of the final redundancy equation is:

$$\hat{} = \cdot \mathbf{P}^{-1} + \mathbf{m}\pi$$

where $\mathbf{m}$ is a vector consist of 0 and 1. Other information must be added to get accurate $\hat{}$.

B. Phase Unwrapping

For the very short baselines, which normally means the shortest and the second shortest baseline, the visibility is mainly determined by Earth/sky and land/sea contours, insensitivity to the brightness temperature details of the Earth disk. So the phase can be predicted in a confidence interval. Thus, the phase ambiguity of these baselines can be easily solved by a comparison between the solution of final redundancy equations and the preset confidence interval.

For other baselines, some techniques should be considered for phase unwrapping. One is closure phase [**?**], which is widely used in optical synthetic aperture field to eliminate the phase error of atmospheric disturbance. For microwave synthetic aperture radiometer, the closure phase relationship can be derived from:

$$\phi_{ab} + \phi_{bc} + \phi_{ca} = \psi_{ab} + \psi_{bc} + \psi_{ca}$$

This can be written in a simplified form as:

$$\phi_{ab} + \phi_{bc} + \phi_{ca} = 0$$

When the first channel is set as a reference by assigning a zero phase to it, Eq. (10) is proved a determined and complete system of equations for solving the unknown phases in a least-square sense as long as the equations related to all adjacent antenna pairs are preserved [**?**]. So the equations corresponding to long baselines should be removed because of serious fringe washing or poor SNR.

In addition, equal length baselines could produce redundancy equations during array rotation [**?**], which can be described as:

$$\phi_{ab}^{\theta} - \phi_{ij}^{\theta} = \alpha_a - \alpha_b - \alpha_i + \alpha_j$$

where baseline ab and baseline ij have the same length. Similar as Eq. (7), running average scheme and long baselines removing are also operated for Eq. (11), the optimized results of all equal length baselines can be written in a simplified form:

$$\hat{\gamma}_{ab-ij} = \alpha_a - \alpha_b - \alpha_i + \alpha_j$$

Baseline superscripts stick to each other in a closed loop, which is so-called phase closure. Eq. (14) implies that, if two of the phase closure have been phase unwrapped, the remaining one will be solved by closure phase relationship.

Another technique is equal length baselines, which has already been involved in final redundancy equations and now is used again for phase unwrapping. For equal length baselines ab and ij, we can get:

$$\phi_{ab} - \phi_{ij} = \alpha_a - \alpha_b - \alpha_i + \alpha_j$$

In which, as one of these equal length baselines has been phase unwrapped, the remaining baselines will be solved.

Eq. (14) and Eq. (15) would also yield large errors due to very poor measurement SNR, which can be optimized by running average scheme similarly as Eq. (7). What should be noticed is that phase unwrapping can only deduce phase ambiguity and has no influence on the solution accuracy, which is decided by the final redundancy equations.

IV. SIMULATION AND EXPERIMENT

A. Geo-image Simulation

In order to assist the implementation of GIMS, a simulator function is developed to calculate the visibility and reconstructed image [**?**]. Pseudo-polar Fast Fourier Transform Algorithm is used in the simulator [**?**].

The original input of simulation is a full Earth imaging at 50.3 GHz, which is shown in Fig. 3(a). The antenna array is shown in Fig. 2(a). After brightness-to-visibility simulation, the maximum visibility amplitudes for each baseline are shown in Fig. 3(b), in which the visibility amplitude drops dramatically with increasing baseline length. Inter-element phase calibration has been conducted with baselines less than 130 . The corresponding visibility amplitude is about 0.25 K.

During inversion simulation, thermal noise with standard deviation corresponding to 500 ms integration time is added to the visibility. Random phase errors within ±40° are added to the receiving elements. The reconstructed image without phase calibration is shown in Fig. 4(a). Annular fuzziness is serious because of the phase error. Snapshot SNR in Eq. (6) and Eq. (11) is just about

4. After optimization by running average scheme, in which the averaging time slice is selected as 5 min, SNR can be improved to larger than 26, which gives a random phase lower than 1.3° with a standard variation of 0.06° K. For the shortest baselines with length 3.1λ and the second shortest baselines with length 6.3λ, the phase will be preset as $[-2\pi, 2\pi]$ and $[-3\pi/2, 3\pi/2]$ respectively. The reconstructed image after inter-element phase calibration is shown in Fig. 4(b).

To evaluate the influence of residual element phase error, radiometric error is defined as the standard deviation of $\Delta T(\xi, \eta)$, which is the difference between the ideal and error-contained retrieved image inside the circle with radius $r = 0.1$, corresponding to the incidence angle of 45° from GEO [?]. Element phase error is defined as the standard deviation of residual element phase error after inter-element phase calibration. Fig. 5 [FIGURE:5] shows radiometric error increase in relation to element phase error. Taking into account an overall radiometric error of 1.5 K, if 0.3 K is assigned to phase errors, residual element phase error must be constrained to 0.9°.

The residual phase error largely depends on the length of averaging time slice for inter-element phase calibration. However, the time length cannot be arbitrarily extended due to changing objective image and instrument stability. After one hundred times of repeating experiments, the relationship between residual element phase error and averaging time is shown in Fig. 6 [FIGURE:6]. 0.9° residual element phase error corresponds to 5 min averaging time.

From Fig. 5, the sensitivity to phase errors has been found to be 0.33° K^{-1}. However, it is known that the radiometric error is mainly contributed by phase errors in the shorter baselines due to the fact that they contain a larger amount of signal energy [?]. After this inter-element phase calibration, the residual baseline phase error is shown in Fig. 7

. It should be noticed that the residual phase error is much better for short baselines because of deliberate consideration in the final redundancy equations, which is important to reduce radiometric error.

B. Field Image Calibration

A proof-of-concept demonstrator with 28 antenna/receiver units has already been achieved for GIMS advanced research [?], as shown in Fig. 8. It has the threshold system performance requirements proposed by application study, in which the image refresh period is 5 mins, and the radiometric accuracy is 1.5 K.

Imaging tests had been conducted for some angularly small targets surrounded by cold sky at a far distance, which is beneficial to suppress aliasing effects. A chosen target is shown in Fig. 9 [FIGURE:9].

The reconstructed image without phase calibration is shown in Fig. 10(a). Improved imaging results have been reported in [?] by using an external point noise source for phase calibration. Here we reprocess the raw data by inter-element

Figure 3: Figure 7

phase calibration approach. The reconstructed image is demonstrated in Fig. 10(b). Compared with Fig. 10(a), the imaging is improved apparently.

V. CONCLUSION

The traditional phase calibration method of noise injection suffers from system complexity and excessive requirements on the calibration of noise injection network itself. In this paper, a new inter-element phase self-calibration method for rotation interferometric radiometers has been introduced, which uses the observation scene as reference without needing extra hardware structure and auxiliary point source.

In the inter-element phase calibration approach, running average scheme is proposed to reduce the effect of noise and phase ambiguity is solved by preset-phase of very short baseline visibility. Simulation and experiments have demonstrated that this method can effectively reduce system phase error.

As future work, some parameters in this new method should be optimized for GIMS and calibration precision should be further quantificationally calculated for the evaluation of sensitivity.

REFERENCES

[1] STAELIN D, GASIEWSKI A, KEREKES J, et al. Concept proposal for a Geostationary Microwave Observatory. Prepared for NASA/NOAA Advanced Geostationary Sensor (AGS) Program, 1998, 23.

[2] BIZZARRI B, GASIEWSKI A, STAELIN D. Initiatives millimetre/submillimetre-wave sounding from geostationary orbit; proceedings of the Geoscience and Remote Sensing Symposium, 2002 IGARSS ' 02 2002 IEEE International, F 2002, 2002.

[3] A. B. Tanner, et al., "Initial Results of the Geostationary Synthetic Thinned Array Radiometer (GeoSTAR) Demonstrator Instrument," IEEE Trans. Geosci. Remote Sens., vol. 45, no. 7, pp. 1947-1957, Jul 2007.

[4] J. Christensen, A. Carlstrom, et al., "GAS: the Geostationary Atmospheric Sounder," in Proc. IGARSS, Barcelona, Spain, 2007.

[5] H. Liu, J. WU, et al., "The Geostationary Interferometric Microwave Sounder (GIMS): instrument Overview and Recent Progress," in Proc. IGARSS, Vancouver, Canada, 2011.

[6] C. Zhang, et al., "Imaging Analysis and First Results of the Geostationary Interferometric Microwave Sounder Demonstrator," IEEE Trans. Geosci. Remote Sens., vol. 53, no. 1, pp. 207-218, Jan 2015.

[7] I. Corbella, et al., "MIRAS end-to-end calibration: application to SMOS L1 processor," IEEE Trans. Geosci. Remote Sens., vol. 43, no. 5, pp. 1126-1134, May 2005.

[8] M. A. Brown, et al., "SMOS Calibration," IEEE Trans. Geosci. Remote Sens., vol. 46, no. 3, pp. 646-658, Mar 2008.

[9] F. Torres, et al., "Analysis of Array Distortion in a Microwave Interferometric Radiometer: Application to the GeoSTAR Project," IEEE Trans. Geosci. Remote Sens., vol. 45, no. 7, pp. 1958-1966, Jul 2007.

[10] R. Jin, et al., "An On-Board External Calibration Method for Aperture Synthesis Radiometer by Rotation," IEEE Trans. Geosci. Remote Sens. Letters, vol. 9, no. 5, pp. 901-905, Sep 2012.

[11] I. Corbella, et al., "The Visibility Function in Interferometric Aperture Synthesis Radiometry," IEEE Trans. Geosci. Remote Sens., vol. 42, no. 8, pp. 1677-1682, Aug 2007.

[12] I. Corbella, et al., "Analysis of Correlation and Total Power Radiometer Front-Ends Using Noise Waves," IEEE Trans. Geosci. Remote Sens., vol. 43, no. 11, pp. 2452-2459, Nov 2005.

[13] R. Butora, "Fringe-washing function calibration in aperture synthesis microwave radiometry," RADIO SCIENCE, vol. 38, no. 2, 2003.

[14] W. J. Fan, et al., "Research of Fourier Phase in Optical Synthetic Aperture Imaging Technique," Acta Optica Sinica, vol. 24, no. 3, Mar 2004.

[15] Y. Zhang, H. Liu, J. Wu, et al., "Target Brightness Temperature Simulation and Analysis for the Geostationary Interferometric Microwave Sounder (GIMS)" in Proc. IGARSS, Milan, Italy, 2015, pp. 3477-3480.

[16] C. Zhang, et al., "Applications of Pseudo-polar FFT in Synthetic Aperture Radiometer Imaging," PIERS online, vol. 3, no. 1, 2007.

[17] F. Torres, A. B. Tanner, et al, "Robust array configuration for a microwave interferometric radiometer: Application to the GeoSTAR project," IEEE Geosci. Remote Sens. Lett., vol. 4, no. 1, pp. 97-101, Jan. 2007.